

## 2.1 $\mu\text{m}$ emission of $\text{Tm}^{3+}/\text{Ho}^{3+}$ – doped antimony-silicate glasses for active optical fibre

J. ŻMOJDA, D. DOROSZ\*, and J. DOROSZ

Faculty of Electrical Engineering, Białystok University of Technology, 45d Wiejska St., 15- 351 Białystok, Poland

**Abstract.**  $\text{Tm}^{3+}/\text{Ho}^{3+}$  – doped antimony-silicate optical fibre with 2.1  $\mu\text{m}$  emission has been presented. Luminescence corresponding to  ${}^5\text{I}_7 \rightarrow {}^5\text{I}_8$  transition in holmium was obtained by energy transfer between  $\text{Tm}^{3+}$  and  $\text{Ho}^{3+}$  ions. The analysis of the luminescence mechanism showed a significant influence of the glass composition (low phonon content) on the emission intensity. Optimization of the active elements content, presented in the paper, allowed to indicate that a strong emission intensity at 2  $\mu\text{m}$  in the fabricated glasses was obtained for the molar composition of 1%  $\text{Tm}_2\text{O}_3$  : 0.75%  $\text{Ho}_2\text{O}_3$ . According to the Förster-Dexter theory, the efficiency of energy transfer of the  ${}^3\text{F}_4$  ( $\text{Tm}^{3+}$ )  $\rightarrow$   ${}^5\text{I}_7$  ( $\text{Ho}^{3+}$ ) transition was calculated. Moreover, it was found that the full width at half maximum (FWHM) of luminescence in the range of 1.6 – 2.2  $\mu\text{m}$  strongly depends on the  $\text{Tm}^{3+}/\text{Ho}^{3+}$  ratio. The optimization of  $\text{Tm}^{3+}/\text{Ho}^{3+}$  transfer in antimony-silicate glasses allowed to fabricate optical fibre with narrowing and red-shifting of emission at 2.1  $\mu\text{m}$ .

**Key words:** antimony-silicate glasses,  $\text{Tm}^{3+}/\text{Ho}^{3+}$  glasses, active optical fibre.

### 1. Introduction

Solid-state lasers emitting radiation at wavelengths of approx. 2  $\mu\text{m}$  are currently an important research subject in many research centres [1–4]. Owing to a strong absorption of radiation by  $\text{OH}^-$  ions within this range, such sources are applied, among others, in medicine [3], remote sensing of the atmospheric composition [5, 6], and DIAL systems [7]. Moreover, radiation exceeding 1.5  $\mu\text{m}$  is widely considered as safe for the eyes, hence the possibility of constructing safe rangefinders and laser radars [8].

Emission in the region of 2  $\mu\text{m}$  is possible through using  $\text{Tm}^{3+}$  or  $\text{Ho}^{3+}$  ions as activators [9, 10]. A direct excitation of  $\text{Tm}^{3+}$  ions from their ground state to the  ${}^3\text{H}_4$  level takes place as a result of radiation absorption, at the maximum wavelength of 795 nm. As a consequence, a quantum transition of  ${}^3\text{F}_4 \rightarrow {}^3\text{H}_6$  ( $\text{Tm}^{3+}$ ) can be observed in the structure of thulium, with a corresponding emission at the wavelength of 1.8  $\mu\text{m}$ . However, in the case of  $\text{Ho}^{3+}$  ions, a lack of commercially available high-power semiconductor diodes which would allow for effective excitation of this element is a significant problem. Therefore, it is necessary to apply sensibilisators in the form of  $\text{Tm}^{3+}$  or  $\text{Yb}^{3+}$  ions. They transfer the absorbed excitation energy, thus making it possible to produce emission at the wavelength of 2  $\mu\text{m}$ , corresponding to the  ${}^5\text{I}_7 \rightarrow {}^5\text{I}_8$  ( $\text{Ho}^{3+}$ ) transition [8].

Literature sources mention a number of glass systems doped with the  $\text{Tm}^{3+}/\text{Ho}^{3+}$  ion systems, in which radiation emissions in the region of 2  $\mu\text{m}$  were obtained [9–10]. These include silicate [11], phosphate [12], HMO (heavy metal oxide) [13], and tellurite glasses [14]. The first two systems are known for their high mechanical resistance and thermal stability required in constructing high-power fibre lasers.

On the other hand, however, these glasses are characterised by a low solubility of rare earths and a high probability of non-radiative transfers caused by high phonon energy (1100–1200  $\text{cm}^{-1}$ ) [11]. Because of that, an alternative to the above glasses can be glasses of low energy of bond oscillation (400–750  $\text{cm}^{-1}$ ), including HMO and tellurite glasses. Besides that, these glasses are capable of hosting relatively great quantities of activator ions, and the phonon transition probability is low. Unfortunately, a consequence of weak structural bonds is a significantly lower (when compared to this of silicate glasses) mechanical strength, which often makes it impossible to produce good quality optical fibres from them [14, 15].

In order to select a composition of glass which would have properties enabling an effective transfer of energy among dopant ions as well as good thermal and mechanical parameters, the best solution is a matrix combining the properties of the two aforementioned groups of glassy materials. As a result of their research, the authors performed a synthesis of antimony-silicate glasses doped with  $\text{Tm}^{3+}$  and  $\text{Ho}^{3+}$  ions to obtain radiation emission within the range of 1.7–2.2  $\mu\text{m}$ . The composition of the core glass in which an effective energy transfer  $\text{Tm}^{3+} \rightarrow \text{Ho}^{3+}$  was observed, was determined by optimization of the content of rare earth ions and the  $\text{Tm}^{3+}/\text{Ho}^{3+}$  ion ratio. The received glass was used for producing double-clad optical fibre whose luminescent parameters were then evaluated.

### 2. Experiments

The  $(44 - x) \text{SiO}_2 - 5\text{Al}_2\text{O}_3 - 50\text{Sb}_2\text{O}_3 - 1\text{Tm}_2\text{O}_3 - x\text{Ho}_2\text{O}_3$  mol% ( $x = 0.1; 0.2; 0.5; 0.75; 1.0; 1.25; 1.5$ ) system were melted in a platinum crucible in an electric fur-

\*e-mail: d.dorosz@pb.edu.pl

nance in temperature of 1550°C for 30 minutes in an argon atmosphere. The molten glass was poured out onto a brass plate and then exposed to the process of annealing in the temperature approximate to the transformation temperature for 12 hours. Homogenous and transparent glasses were obtained without visible effect of crystallization. In order to determine spectral properties a series of samples with the dimensions of  $8 \times 8 \times 3 \text{ mm}^3$  were prepared. The spectral transmission measurement within the range from 0.5 to 1.7  $\mu\text{m}$  was taken using an Acton Spectra Pro 2300i monochromator with an InGaAs detector. The glass density  $\rho$  was calculated using the method of hydrostatic weighing. The refractive index (633 nm) was determined with the aid of a Metricon 2010 refractometer. The characteristic temperatures of the obtained glasses were calculated based on the measurement taken with a SETARAM Labsys thermal analyzer using the DSC method. The luminescence spectrum within the range from 1550 to 2300 nm was measured at a station equipped with a Stelarnet RW-InGaAs-1024X spectrometer and a laser diode ( $\lambda_p = 795 \text{ nm}$ ) with an optical fibre output having the maximum optical power  $P = 30 \text{ W}$ .

### 3. Results

The results of measurements on physico-chemical properties of the produced glasses are shown in Table 1. A combination of two elements, silicon and antimony, of extremely different bond energy, led to obtaining thermally stable and mechanically strong glasses of a wide range of transmission spectra (0.3–3.5  $\mu\text{m}$ ) in the order of 95%. The low phonon energy of the obtained antimony glasses ( $650 \text{ cm}^{-1}$ ) made it possible to introduce significant amounts of rare earth elements (25000 ppm) to the structure. Furthermore, antimony-silicate glasses are characterised by a high coefficient of light refraction (1.74), which is the reason for the high value of the emission cross-section.

Table 1  
Physico-chemical properties of antimony-silicate glasses

Parameter	Value
Refractive index $n$ (at 633 nm)	1.74
Mass density $\rho$ [ $\text{g}/\text{cm}^3$ ]	3.12
Transmission range [ $\mu\text{m}$ ]	0.3–3.5
Transformation temperature [ $^{\circ}\text{C}$ ] (DSC)	475
Concentration of all active ions $N$ [ $10^{20} \text{ ion}/\text{cm}^3$ ]	3.5
Average interionic radius $R$ [ $\text{\AA}$ ]	8.42

In the obtained glasses, the  $N$  concentration of the introduced active ions, at which no effect of clustering was observed, amounts to  $3.5 \times 10^{20} \text{ [ion}/\text{cm}^3]$ . On the basis of this value ( $N = N_{Tm} + N_{Ho}$ ), the average interionic distance defined as  $R = (3/4\pi N)^{1/3}$  was determined. The knowledge of the distances between atoms of Tm and Ho ions makes it possible to interpret processes which take place in glasses codoped with rare earth ions, applying the Förster-Dexter semi-empirical model [16, 17]. According to this model, the probability of non-radiative and resonance energy transfer among

ions, considering the multipolar character of the interaction, can be described by the following dependence [18]:

$$W_{DA} = \frac{1}{\tau_D} \left[ \left( \frac{R_0}{R} \right)^6 + \left( \frac{R_0}{R} \right)^8 + \left( \frac{R_0}{R} \right)^{10} \right], \quad (1)$$

where  $\tau_D$  – the donor lifetime,  $R$  – the average distance between the donor and the acceptor,  $R_0$  – the critical interionic distance at which the probability of energy transfer between the donor and the acceptor and the probability of the process of radiative relaxation of the donor are equal.

Depending on the range of its influence, the  $R_0$  distance is described in the following way:

- for dipole-dipole interactions,

$$R_0^6 = \frac{3h^4 c^4}{4\pi n^4} Q_A \int \frac{f_D(E) f_A(E)}{E^4} dE, \quad (2)$$

- for dipole-quadrupole interactions,

$$R_0^8 = \frac{135\pi h^9 c^8}{4n^6} Q_A \int \frac{f_D(E) f_A(E)}{E^8} dE, \quad (3)$$

- for quadrupole-quadrupole interactions,

$$R_0^{10} = \frac{225\pi h^{11} c^{10}}{2n^6} Q_A \int \frac{f_D(E) f_A(E)}{E^{10}} dE \quad (4)$$

where  $f_D(E)$ ,  $f_A(E)$  are normalised distributions of the donor emission and the acceptor absorption cross-sections,  $n$  is the coefficient of light refraction in the material,  $Q_A$  is the oscillator strength of the absorption band which is in resonance with the donor emission transition, and  $E$  is the average photon energy.

The total probability of energy transfer in each case is directly dependent on the overlap integral of the spectra, and it is inversely proportional to the average distance between the interacting ions [19].

**Absorption coefficient.** On the basis of the conducted measurements of spectral transmission and of the (5) dependence, absorption coefficients for the received glasses activated with two lanthanides were determined.

$$\alpha(\lambda) = \frac{1}{d} \ln \left( \frac{1}{T_r(\lambda)} \right). \quad (5)$$

Figure 1 presents absorption spectra for glasses doped with  $\text{Tm}^{3+}$  as well as  $\text{Tm}^{3+}$  and  $\text{Ho}^{3+}$  ions. In glasses doped with thulium ions, absorption bands corresponding to transitions from the  $^3\text{H}_6$  ground state to higher energetic levels of  $^3\text{F}_4$ ,  $^3\text{H}_5$ ,  $^3\text{H}_4$ , and  $^3\text{F}_{2,3}$  were observed. Additional introduction of holmium ions to the matrix leads to the appearance of absorption bands resulting from the quantum structures of energetic levels in holmium ions. After having studied the changes in the absorption curve, five bands corresponding to transitions from the  $^5\text{I}_8 \rightarrow ^5\text{I}_7$ ,  $^5\text{I}_6$ ,  $^5\text{I}_5$ ,  $^5\text{F}_5$  level were identified. The absorption levels for the respective bands in holmium ions increase together with increased activator concentrations, whereas the spectral positions of transition maxima remain constant. The presented absorption curve pertains to the glass which was doped at the ratio of 1% $\text{Tm}_2\text{O}_3$ :0.75% $\text{Ho}_2\text{O}_3$ .

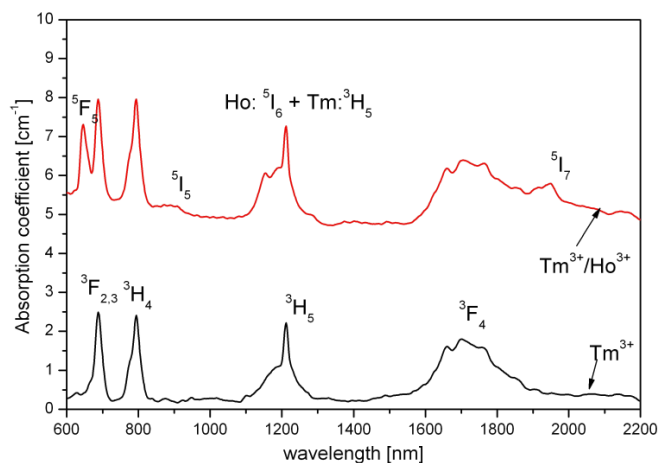
2.1  $\mu\text{m}$  emission of  $\text{Tm}^{3+}/\text{Ho}^{3+}$  – doped antimony-silicate glasses for active optical fibre

 Fig. 1. Absorption spectra of glasses doped with  $\text{Tm}^{3+}$  and  $\text{Tm}^{3+}/\text{Ho}^{3+}$  ions

Table 2 illustrates basic parameters, i.e. the wavelength at the  $\lambda$  maximum absorption transition, the  $\Delta\lambda$  spectral range of the absorption band, and the average energy.

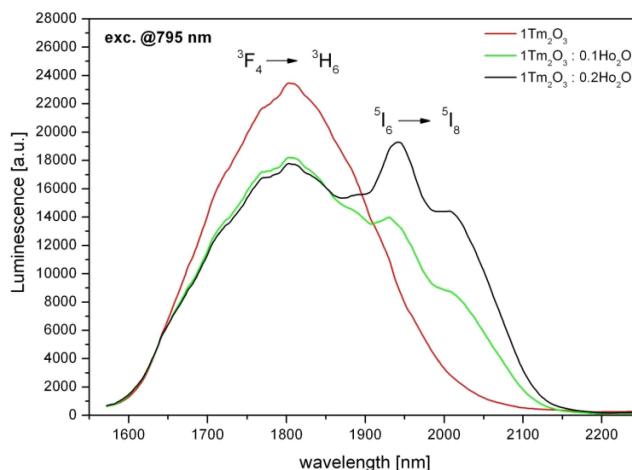
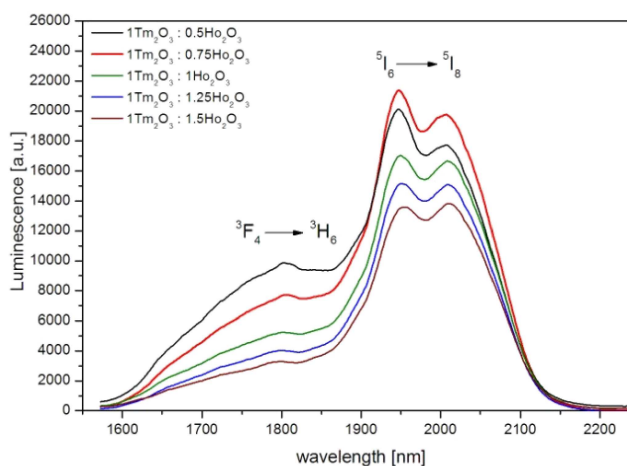
 Table 2  
 Absorption parameters of singly doped glasses

Transition	$\Delta\lambda[\text{nm}]$	$\lambda[\text{nm}]$	$E[\text{cm}^{-1}]$
${}^3\text{H}_6 \rightarrow {}^3\text{F}_{2,3}$	658–710	688	14534
${}^3\text{H}_4$	762–818	794	12594
${}^3\text{H}_5$	1134–1262	1212	8250
${}^3\text{F}_4$	1580–1890	1712	5841
Transition	$\Delta\lambda[\text{nm}]$	$\lambda[\text{nm}]$	$E[\text{cm}^{-1}]$
${}^5\text{I}_8 \rightarrow {}^5\text{F}_5$	630–670	644	15527
${}^5\text{I}_5$	878–918	898	11135
${}^5\text{I}_6$	1120–1240	1155	8658
${}^5\text{I}_7$	1820–2105	1950	5128

**Luminescence properties.** The obtained glasses doped with  $\text{Tm}^{3+}$  as well as  $\text{Tm}^{3+}$  and  $\text{Ho}^{3+}$  ions were excited by radiation of the wavelength of 795 nm, due to the strong  ${}^3\text{H}_6 \rightarrow {}^3\text{H}_4$  ( $\text{Tm}^{3+}$ ) transition absorption. As a result, luminescence lines in the range of 1.6–2.2  $\mu\text{m}$  were observed. Figure 2 shows the obtained luminescence spectra for glasses activated with 1%  $\text{Tm}_2\text{O}_3$  and for glasses doped at the ratios of 1%  $\text{Tm}_2\text{O}_3$ :0.1 $\text{Ho}_2\text{O}_3$  and 1%  $\text{Tm}_2\text{O}_3$ :0.2% $\text{Ho}_2\text{O}_3$ . The produced samples doped exclusively with thulium ions are characterised by strong luminescence lines with maxima at the wavelength of 1836 nm equivalent to the quantum transition of  ${}^3\text{F}_4 \rightarrow {}^3\text{H}_6$ . Introducing holmium ions to glass results in a decrease of the level of luminescence coming from  $\text{Tm}^{3+}$  ions; at the same time, a strong emission line appears in the region of 2  $\mu\text{m}$  corresponding to the  ${}^5\text{I}_7 \rightarrow {}^5\text{I}_8$  transition in the energetic structure of holmium ions.

As a result, a significant broadening of the luminescence spectrum, caused by overlapping of the  ${}^3\text{F}_4 \rightarrow {}^3\text{H}_6$  ( $\text{Tm}^{3+}$ ) and  ${}^5\text{I}_7 \rightarrow {}^5\text{I}_8$  ( $\text{Ho}^{3+}$ ) emission transitions was observed in the glass which was doped at the ratio of 1%

$\text{Tm}_2\text{O}_3$  : 0.2%  $\text{Ho}_2\text{O}_3$ . The full width at half maximum of the ( $\text{Tm}/\text{Ho}$ ) emission amounts to 356 nm, and for the glass doped with  $\text{Tm}^{3+}$  ions FWHM = 238 nm. Increasing the molar concentration of holmium ions leads to decreasing luminescence of the  ${}^3\text{F}_4 \rightarrow {}^3\text{H}_6$  ( $\text{Tm}^{3+}$ ) transition and to the appearance of a strong luminescence line in the region of 2  $\mu\text{m}$  (Fig. 3).

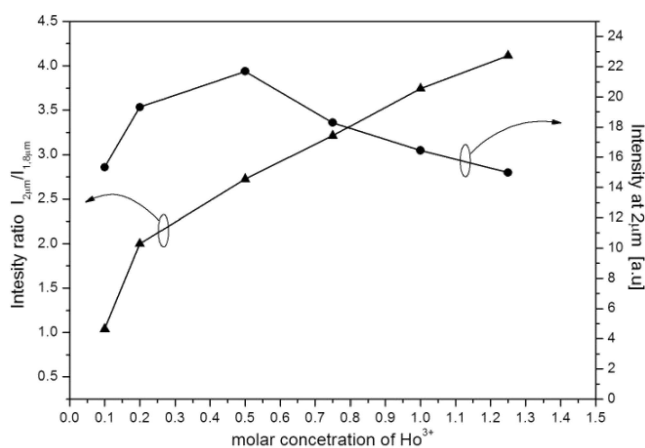

 Fig. 2. Luminescence spectra for glasses doped with  $\text{Tm}^{3+}$  and  $\text{Tm}^{3+}/\text{Ho}^{3+}$  ions

 Fig. 3. Luminescence spectra of glasses doped with  $\text{Tm}^{3+}/\text{Ho}^{3+}$  ions with increasing holmium ratio

The decrease in the intensity of the luminescence line for the  ${}^3\text{F}_4 \rightarrow {}^3\text{H}_6$  ( $\text{Tm}^{3+}$ ) transition is therefore connected with transferring some amount of energy through non-radiative transfer between thulium and holmium ions. Figure 3 illustrates the dependence of the emission intensity at the wavelength of approx. 2  $\mu\text{m}$  on the concentration of holmium ions. An increase in the  ${}^5\text{I}_7 \rightarrow {}^5\text{I}_8$  ( $\text{Ho}^{3+}$ ) transition luminescence is observed up to the molar concentration of 0.5 mol%  $\text{Ho}_2\text{O}_3$ . After this concentration is exceeded, a linear decrease in the emission intensity takes place, possibly as a result of diffusion transitions of the donor-donor type or concentration quenching.

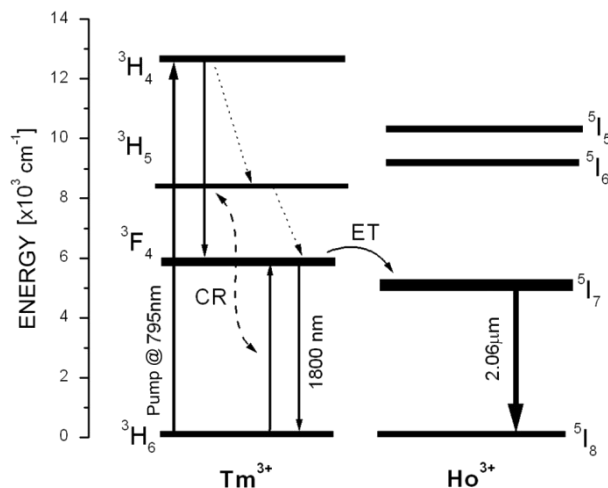
Table 3  
 The FWHM, 2 $\mu\text{m}$  intensity and intensity ratios of luminescence bands

Parameter	Glass sample							
	1Tm <sub>2</sub> O <sub>3</sub>	1Tm <sub>2</sub> O <sub>3</sub> : 0.1Ho <sub>2</sub> O <sub>3</sub>	1Tm <sub>2</sub> O <sub>3</sub> : 0.2Ho <sub>2</sub> O <sub>3</sub>	1Tm <sub>2</sub> O <sub>3</sub> : 0.5Ho <sub>2</sub> O <sub>3</sub>	1Tm <sub>2</sub> O <sub>3</sub> : 0.75Ho <sub>2</sub> O <sub>3</sub>	1Tm <sub>2</sub> O <sub>3</sub> : 1Ho <sub>2</sub> O <sub>3</sub>	1Tm <sub>2</sub> O <sub>3</sub> : 1.25Ho <sub>2</sub> O <sub>3</sub>	1Tm <sub>2</sub> O <sub>3</sub> : 1.5Ho <sub>2</sub> O <sub>3</sub>
FWHM	238	310	356	184	178	178	182	180
I <sub>2<math>\mu\text{m}</math></sub>	–	8.53	14.29	17.66	19.68	16.80	15.23	13.99
I <sub>2<math>\mu\text{m}</math></sub> /I <sub>1.8<math>\mu\text{m}</math></sub>	–	0.45	0.77	1.73	2.47	3.12	3.71	4.19

Figure 4 demonstrates the influence of Ho<sup>3+</sup> ion concentration on changes in the ratio of the intensity of the luminescence line coming from I<sub>2 $\mu\text{m}$</sub>  holmium ions to the intensity of luminescence for I<sub>1.8 $\mu\text{m}$</sub>  thulium ions. The curve indicates that introducing the acceptor ions (Ho<sup>3+</sup>) induces a nearly four-fold increase of the I<sub>2 $\mu\text{m}$</sub> /I<sub>1.8 $\mu\text{m}$</sub>  ratio and proves that an effective transfer of some energy between Tm<sup>3+</sup> and Ho<sup>3+</sup> ions takes place (Table 3).


 Fig. 4. Influence of Ho<sup>3+</sup> ion concentration on the intensity changes of the luminescence

**Mechanism of ET.** The presence in the glassy matrix of various rare earth elements which act as donors and acceptors, can lead to such processes as: ground-state absorption (GSA), excited-state absorption (ESA), energy transfer (ET), cross relaxation (CR), multiphonon relaxation (MPR), and photon emission [20]. An analysis of the occurrence of the above effects in the produced matrix makes it possible to optimize both the glass composition and the concentration of active dopants. In the case under research, the mechanism of a non-radiative resonance energy transfer between excited metastable levels of Tm<sup>3+</sup> (<sup>3</sup>F<sub>4</sub>) and Ho<sup>3+</sup> (<sup>5</sup>I<sub>7</sub>) ions is presented in Fig. 5. In thulium ions, optical pumping (795 nm) results in the population of the <sup>3</sup>H<sub>4</sub> level which enables transfer to lower energetic levels: <sup>3</sup>H<sub>5</sub> and <sup>3</sup>F<sub>4</sub>. The <sup>3</sup>H<sub>5</sub> level in thulium is characterised by a short lifetime and its role in the relaxation process can be neglected, whereas the lifetime of the <sup>3</sup>F<sub>4</sub> level is long, and as a result it allows for reaching a high population density at this level.


 Fig. 5. Mechanism of a non-radiative resonance energy transfer between Tm<sup>3+</sup> and Ho<sup>3+</sup>

The population of the <sup>3</sup>F<sub>4</sub> level occurs mainly as an effect of the processes of non-radiative and cross relaxation whose contribution depends on the glass type [21]. It has to be emphasised that the probability of multi-phonon transfers in matrices of low oscillation energy is minimal [22]. Therefore, the population of the <sup>3</sup>F<sub>4</sub> level in the obtained antimony glasses takes place mainly in the cross relaxation process, according to the following mechanism: <sup>3</sup>H<sub>4</sub>(Tm<sup>3+</sup>) + <sup>3</sup>H<sub>6</sub>(Tm<sup>3+</sup>) → <sup>3</sup>F<sub>4</sub>(Tm<sup>3+</sup>) + <sup>3</sup>F<sub>4</sub>(Tm<sup>3+</sup>). The subsequent holmium doping leads to an energy transfer between the <sup>3</sup>F<sub>4</sub>(Tm<sup>3+</sup>) → <sup>5</sup>I<sub>7</sub>(Ho<sup>3+</sup>) energetic levels. This process can be characterised by determining spectral cross sections of absorption for holmium as well as those of emission for thulium ions, which allows for determining the distances between the dopant atoms. The degree of spectral matching between cross-sections is closely related to the probability of energy migration between the excited levels of the two elements. In practice, the probability of the energy exchange process is inversely proportional to R<sup>6</sup> for dipole-dipole interactions and to R<sup>8</sup> for dipole-quadrupole interactions. An increase in the Ho<sup>3+</sup> ions concentration affects a decrease in the distances between two coupled ions, and energy migration at excited levels increases. As a consequence, this leads to increasing the probability of energy transfer. The process performance is, however, limited by the back electron transfer (BET) whose probability is high, especially for resonant interactions. The BET process depends decisively on multiphonon transfers (MPR) and grows together with an increase in the

## 2.1 $\mu\text{m}$ emission of $\text{Tm}^{3+}/\text{Ho}^{3+}$ – doped antimony-silicate glasses for active optical fibre

phonon energy in the matrix structure [23]. Figure 6 illustrates the  ${}^3\text{F}_4(\text{Tm}^{3+}) \rightarrow {}^5\text{I}_7(\text{Ho}^{3+})$  energy transfer efficiency in the function of the content of the  $(\text{Ho}^{3+})$  acceptor ions for the analysed system.

The energy transfer efficiencies between the donor and the acceptor were calculated on the basis of analysing changes in the quantum leap of  ${}^3\text{F}_4 \rightarrow {}^3\text{H}_6$  in glasses doped with thulium as well as with thulium and holmium ions. A dependence developed on the basis of the Förster theory was applied for that purpose [16]:

$$\eta = 1 - \frac{I_{TmHo}}{I_{Tm}}, \quad (6)$$

where  $I_{TmHo}$  – luminescence intensity in  $\text{Tm}^{3+}/\text{Ho}^{3+}$  glasses,  $I_{Tm}$  – luminescence intensity in  $\text{Tm}^{3+}$  glasses.

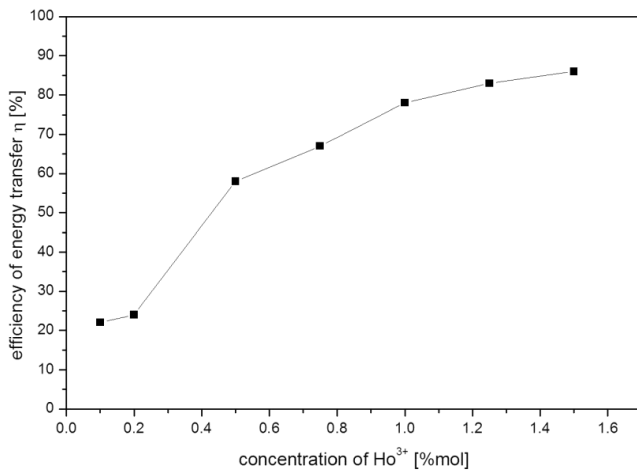


Fig. 6. Efficiency of energy transfer  ${}^3\text{F}_4(\text{Tm}^{3+}) \rightarrow {}^5\text{I}_7(\text{Ho}^{3+})$  vs.  $\text{Ho}^{3+}$  ions content

Optimization of the process of resonance energy transfer between thulium and holmium ions was based on calculating the absorption and emission cross-sections. Dependencies (7) and (8) describe the  $\sigma_{abs}$  absorption cross-section and the  $\sigma_{em}$  stimulated emission cross-section, calculated respectively using the Lambert-Beer law [24] and the McCumber theory [25]:

$$\sigma_{abs}(\lambda) = \frac{2.303 \log(1/T(\lambda))}{dN}, \quad (7)$$

$$\begin{aligned} \sigma_{em}(\lambda) &= \sigma_{abs}(\lambda) K \exp\left(\frac{E_0 - \frac{hc}{\lambda}}{kT}\right) = \\ &= \sigma_{abs}(\lambda) \frac{Z_{low}}{Z_{up}} \exp\left(\frac{hc}{kT} \left(\frac{1}{\lambda_p} - \frac{1}{\lambda}\right)\right), \end{aligned} \quad (8)$$

where  $T(\lambda)$  – spectral transmission,  $N$  – lanthanides concentration [ion/ $\text{cm}^3$ ],  $d$  – sample thickness,  $Z_{low}$  and  $Z_{up}$  are corresponding partition functions of lower (low) and upper (up) multiplets, respectively [25]. On the basis of an energy diagram,  $E_0$  was also determined; its value corresponds to the energy difference between the lowest Stark levels of the ground and excited states, between which emission at the wavelength of  $\lambda_p$  takes place.

The calculated ( ${}^5\text{I}_8 \rightarrow {}^5\text{I}_7$ ) holmium ions absorption and ( ${}^3\text{F}_4 \rightarrow {}^3\text{H}_6$ ) thulium ions emission cross-sections can be seen in Fig. 7. The value of the emission cross-section for the  ${}^3\text{F}_4 \rightarrow {}^3\text{H}_6$  ( $\text{Tm}^{3+}$ ) transfer, corresponding to the wavelength of  $\lambda_p = 1818$  nm, amounts to  $\sigma_{em} = 9.1 \times 10^{-21} \text{ cm}^2$ , which means it is significantly higher than the values of emission cross-sections for silicate glasses [26], ZBLAN [27], tellurite [30] and similar to these for germanium glasses [28, 29].

The high cross-section values for the fabricated glasses are connected to a high coefficient of the light refraction of the matrix. Moreover, high values of the  $\sigma_{abs} = 5.65 \times 10^{-21} \text{ cm}^2$  absorption cross-section at the wavelength of 794 nm ( ${}^3\text{H}_6 \rightarrow {}^3\text{H}_4$ ) in glasses doped with thulium ions ensure effective population of the  ${}^3\text{H}_4$  level from which energy is subsequently transferred to holmium ions in the processes of cross relaxation  ${}^3\text{H}_4(\text{Tm}^{3+}) + {}^3\text{H}_6(\text{Tm}^{3+}) \rightarrow {}^3\text{F}_4(\text{Tm}^{3+}) + {}^3\text{F}_4(\text{Tm}^{3+})$  and energy transfer  ${}^3\text{F}_4(\text{Tm}^{3+}) \rightarrow {}^5\text{I}_7(\text{Ho}^{3+})$ .

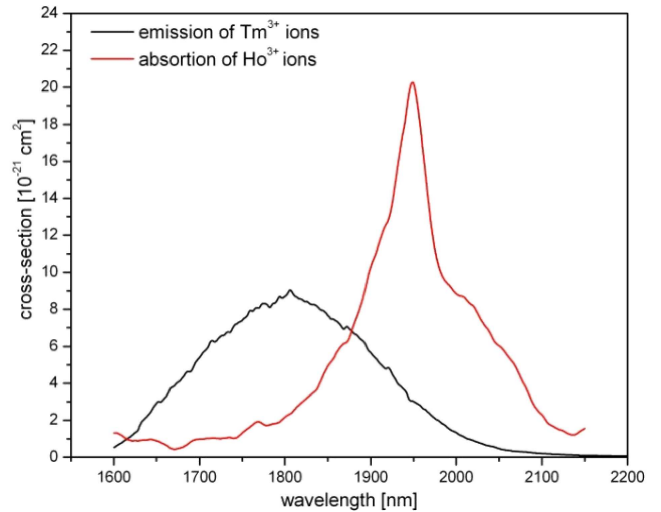


Fig. 7.  $\text{Ho}^{3+}$  ( ${}^3\text{F}_4 \rightarrow {}^3\text{H}_6$ ) absorption and  $\text{Tm}^{3+}$  ( ${}^3\text{F}_4 \rightarrow {}^3\text{H}_6$ ) emission cross-sections

### Double-clad optical fibre doped with $\text{Tm}^{3+}/\text{Ho}^{3+}$ ions.

Antimony-silicate glass of the following molar composition:  $43.25\text{SiO}_2 - 5\text{Al}_2\text{O}_3 - 50\text{Sb}_2\text{O}_3 - 1\text{Tm}_2\text{O}_3 - 0.75\text{Ho}_2\text{O}_3$  was used as the core of the double-clad optical fibre produced using the crucible method. In order to increase the efficiency of optical pumping, the optical fibre core was placed eccentrically in the inner cladding, thus obtaining a system of the off-set type. Selecting the cladding glasses made it possible to obtain the core numeric aperture  $\text{NA}_{core} = 0.2$  and the inner cladding numeric aperture  $\text{NA}_{cladding} = 0.6$ . The obtained optical fibre was excited from the front by a laser diode of the wavelength of 795 nm, as a result of which a strong luminescence line in the region of  $2.1 \mu\text{m}$  was registered (Fig. 8). Strong absorption of some radiation by  $\text{Ho}^{3+}$  atoms was observed in the spectrum. As a result of this absorption, the maximum of the luminescence spectrum shifted to the longer wavelengths. Furthermore, a disappearance of the band characteristic of holmium ions at the wavelength of approx.  $1.95 \mu\text{m}$  was observed in the optical fibre, which in conse-

quence caused a reduction in the full width at half maximum (FWHM = 100 nm) of the emission.

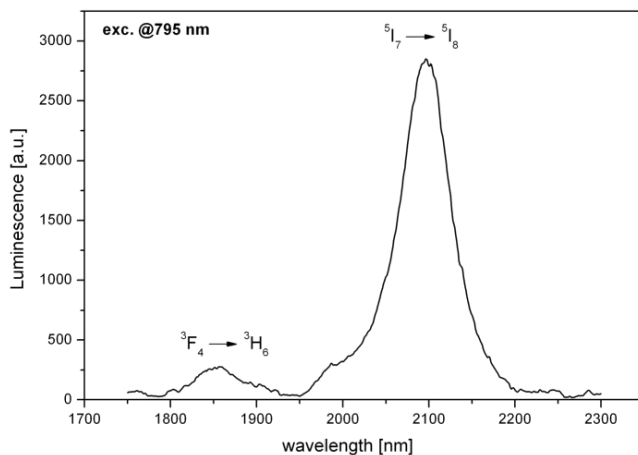


Fig. 8. Luminescence of double-clad optical fibre doped with  $1\text{Tm}_2\text{O}_3\text{-}0.75\text{Ho}_2\text{O}_3$

The strong luminescence at the wavelength of  $2.1\ \mu\text{m}$ , obtained as a result of excitation of thulium ( ${}^3\text{H}_6 \rightarrow {}^3\text{H}_4$ ) in the optical fibre with radiation of the wavelength of  $795\ \text{nm}$ , proves that an effective non-radiative energy transfer between  $\text{Tm}^{3+}$  and  $\text{Ho}^{3+}$  ions occurs in the produced fibre.

#### 4. Conclusions

The present paper describes low-phonon antimony-silicate glasses in which combining glass-making elements of significantly different bond energy led to obtaining thermally stable and mechanically strong glasses of a wide range of transmission spectra ( $0.3\text{--}3.5\ \mu\text{m}$ ) in the order of 95%. The low phonon energy of the produced antimony glasses made it possible to introduce a large quantity (25000 ppm) of rare earth elements to the structure. In effect, it enabled the matrix to be doped with both  $\text{Tm}^{3+}$  and  $\text{Ho}^{3+}$  ions, producing luminescence in the range of  $1.6\text{--}2.2\ \mu\text{m}$ . In glasses doped at the ratio of  $1\% \text{Tm}_2\text{O}_3\text{:}0.2\% \text{Ho}_2\text{O}_3$ , a significant widening of the luminescence spectrum, caused by overlapping of the  ${}^3\text{F}_4 \rightarrow {}^3\text{H}_6$  ( $\text{Tm}^{3+}$ ) and  ${}^5\text{I}_7 \rightarrow {}^5\text{I}_8$  ( $\text{Ho}^{3+}$ ) emission transitions was observed, and the full width at half maximum of the emission was  $356\ \text{nm}$ . Optimization of the content of activators and of the donor ( $\text{Tm}^{3+}$ ) to acceptor ( $\text{Ho}^{3+}$ ) ion concentration ratio, performed taking into consideration the most effective energy transfer, allowed for selecting the glass which was subsequently used for fabricating optical fibre of the double-clad type. In the produced optical fibre, a strong luminescence at the wavelength of  $2.1\ \mu\text{m}$  was obtained, arising from the energy transfer between  $\text{Tm}^{3+}$  and  $\text{Ho}^{3+}$  ions, as a result of excitation of thulium ions ( ${}^3\text{H}_6 \rightarrow {}^3\text{H}_4$ ) with radiation of the wavelength of  $795\ \text{nm}$ .

**Acknowledgements.** This work was supported by Ministry of Science and High Education of Poland – grant No. N N507 285636.

#### REFERENCES

- [1] M. Eichhorn, “Quasi-three-level solid-state lasers in near and mid infrared based on trivalent rare earth ions”, *Appl. Phys. B* 93, 269–316 (2008)
- [2] B.M. Walsch, “Review of Tm and Ho Materials”, *Spectroscopy and Lasers, Laser Physics* 19 (4), 855–866 (2009).
- [3] A. Godard, “Infrared ( $2\text{--}12\ \mu\text{m}$ ) solid-state laser sources: a review”, *C. R. Physique* 8, 1100–1128 (2007).
- [4] A. Zając, D. Dorosz, M. Kochanowicz, M. Skórczakowski, and J. Świdorski, “Fibre lasers – conditioning constructional and technological”, *Bull. Pol. Ac.: Tech* 58 (4), 491–502 (2010).
- [5] D. Milanese, M. Vota, Q. Chen, J. Xing, G. Liao, H. Gebavi, M. Ferraris, N. Coluccelli, and S. Taccheo, “Investigation of infrared emission and lifetime in Tm-doped  $75\text{TeO}_2\text{:}20\text{ZnO:}5\text{Na}_2\text{O}$  (mol%) glasses: effect of Ho and Yb co-doping”, *J. Non-Cryst. Solid* 354, 1955–1961 (2008).
- [6] T. Pustelny, C. Tyszkiewicz, and K. Barczak, “Optical fiber sensors of magnetic field applying Faraday’s effect”, *Optica Applicata* 32 (2–3), 469–475 (2003).
- [7] R. Balda, J. Fernández, S.G. Revilla, and J.M. Navarro, *Opt. Express* 15, 6750 (2007).
- [8] J. G. Bünzli and SvV. Eliseeva, “Lanthanide NIR luminescence for telecommunications, bioanalyses and solar energy conversion”, *J. Rare Earths* 28 (6), 824 (2010).
- [9] M. Wanga L. Yi, G. Wanga, L. Hua, and J. Zhanga, “ $2\ \mu\text{m}$  emission performance in  $\text{Ho}^{3+}$  doped fluorophosphate glasses sensitized with  $\text{Er}^{3+}$  and  $\text{Tm}^{3+}$  under  $800\ \text{nm}$  excitation”, *Solid State Communications* 149, 1216–1220 (2009).
- [10] B. Richards, S. Shen, A. Jha, Y. Tsang, and D. Binks, “Infrared emission and energy transfer in  $\text{Tm}^{3+}$ ,  $\text{Tm}^{3+}\text{-Ho}^{3+}$  and  $\text{Tm}^{3+}\text{-Yb}^{3+}$ -doped tellurite fibre”, *Opt. Express* 15, 6546 (2007).
- [11] S.D. Jackson and S. Mossman, “High-power diode-cladding-pumped  $\text{Tm}^{3+}$ ,  $\text{Ho}^{3+}$ -doped silica fibre laser”, *Appl. Phys. B* 77, 489–493 (2003).
- [12] B. Peng and T. Izumitani, “Blue, green and  $0.8\ \mu\text{m}$   $\text{Tm}^{3+}$ ,  $\text{Ho}^{3+}$  doped upconversion laser glasses, sensitized by  $\text{Yb}^{3+}$ ”, *Opt. Mater.* 4, 797–799 (1995).
- [13] D.M. Shi, Q.Y. Zhang, G.F. Yang, and Z.H. Jiang, “Spectroscopic properties and energy transfer in  $\text{Ga}_2\text{O}_3\text{-Bi}_2\text{O}_3\text{-PbO-GeO}_2$  glasses codoped with  $\text{Tm}^{3+}$  and  $\text{Ho}^{3+}$ ”, *J. Non-Cryst. Solids* 353, 1508–1514 (2007).
- [14] Y. Tsang, B. Richards, D. Binks, J. Lousteau, and A. Jha, “A  $\text{Yb}^{3+}/\text{Tm}^{3+}/\text{Ho}^{3+}$  triply-doped tellurite fibre laser”, *Opt. Express*. 16 (14), 10690–10695 (2008).
- [15] T. Pustelny, K. Barczak, K. Gut, and J. Wojcik, “Special optical fiber type D applied in optical sensor of electric currents”, *Optica Applicata* 34 (4), 531–539 (2004).
- [16] T. Förster, “Zwischenmolekulare Energiewanderung und Fluoreszenz”, *Ann. Physik* 6 (2), 55–59 (1948).
- [17] D.L. Dexter, “A theory of sensitized luminescence in solids”, *J. Chem. Phys.* 21, 836–850 (1953).
- [18] S. Hijanosa and M.A. Meneses-Nava, “Energy back transfer, migration and energy transfer (Yb-to-Er and Er-to-Yb) processes in Yb, Er:YAG”, *J. Lum.* 102–103, 694–698 (2003).
- [19] G.A. Kumar and R.E. Riman, “Near-infrared optical characteristics of chalcogenide-bound  $\text{Nd}^{3+}$  molecules and clusters”, *Chem. Mater.* 19, 2937–2946 (2007).
- [20] M.J.F. Digonet, *Rare-Earth-Doped Fiber Lasers and Amplifiers*, Chapter 2, pp. 17–25, Marcel Dekker, New York, 2001.

*2.1  $\mu\text{m}$  emission of  $\text{Tm}^{3+}/\text{Ho}^{3+}$  – doped antimony-silicate glasses for active optical fibre*

- [21] G. Gao, G. Wang, C. Yu, J. Zhang, and L. Hu, “Investigation of 2.0  $\mu\text{m}$  emission in  $\text{Tm}^{3+}$  and  $\text{Ho}^{3+}$  codoped oxyfluoride tellurite glass”, *J. Lum.* 129, 1042–1047 (2009)
- [22] S.D. Jackson, M. Pollnau, “Mid-infrared fiber lasers”, *Appl. Phys.* 89, 219 – 255 (2003)
- [23] X. Li, Q. Nie, S. Dai, T. Xu, X. Shen, and X. Hang, “Investigation of energy transfer and frequency upconversion in  $\text{Ho}^{3+}/\text{Yb}^{3+}$  co-doped tellurite glasses”, *J. Phys. Chem. Solids* 68 (8), 1566–1570 (2007).
- [24] J. Koetke and G. Huber, “Infrared excited-state absorption and stimulated-emission cross sections of  $\text{Er}^{3+}$ -doped crystals”, *Appl. Phys. B* 61, 151–158 (1995).
- [25] D.E. McCumber, “Einstein relations connecting broadband emission and absorption spectra”, *Physics. Review* 136, A954–A957 (1964).
- [26] B.M. Walsh and N.P. Barnes, “Comparison of Tm: ZBLAN and Tm: silica fiber lasers; spectroscopy and tunable pulsed laser operation around 1.9  $\mu\text{m}$ ”, *Appl. Phys. B* 78, 325–333 (2004).
- [27] J.L. Doualan, S. Girard, H. Haquin, J.L. Adam, and J. Montagne, “Spectroscopic properties and laser emission of Tm doped ZBLAN glass at 1.8  $\mu\text{m}$ ”, *Opt. Mat.* 24, 563–574 (2003).
- [28] H. Fan, G. Gao, G. Wang, J. Hu, and L. Hu, “ $\text{Tm}^{3+}$  doped  $\text{Bi}_2\text{O}_3\text{-GeO}_2\text{-Na}_2\text{O}$  glasses for 1.8  $\mu\text{m}$  fluorescence”, *Opt. Mat.* 32, 627–631 (2010).
- [29] R.R. Xu, Y. Tian, M. Wang, L.L. Hu, and J.J. Zhang, “Spectroscopic properties of 1.8  $\mu\text{m}$  emission of thulium ions in germanate glass”, *Appl. Phys. B* 102, 109–116 (2010).
- [30] M. Reben, J. Wasylak, and J. Jaglarz, “Influence of active admixtures onto tellurite glass refractive index”, *Bull. Pol. Ac.: Tech.* 58 (4), 519–522 (2010).